Design of Protocol Based V2V Emergency DC Fast Charging

[1]K.Sushita, [2]Dr.N.Shanmugasundaram, [3]Dr.T.Thandapani

[1]Assistant Professor, Electrical and Electronics Engineering ,Vels Institute of Science, Technology and advanced Studies, Chennai, India, sushita.se@velsuniv.ac.in

[2]Associate Professor, Electrical and Electronics Engineering ,Vels Institute of Science, Technology and advanced Studies, Chennai, India, shanmugam71.se@velsuniv.ac.in

[3] Director Technical , RRT Electro Powwer (P) Ltd,Chennai, India,epower3@gmail.com

Abstract.

It has been quite some time Electric Vehicles (EV) started plying on the roads and are replacing fossil fuel vehicles. Charging infrastructure is already in place at many cities and highways for hassle free charging. Two types of chargers are deployed. AC and DC chargers, AC Charger utilizes the ON-Board charger of the EV and takes 6 to 8 hours for full charge whereas DC Fast Chargers (DCFC) charges the vehicle within a short period of 20 to 60 minutes. Most AC chargers are installed in apartments, parking lots, offices and malls and are mainly used for topping up. A well implemented charging infrastructure will have a DC charger at every 5 kms within city and a charger on every 25 km on highways. Therefore there is a rare possibility of EV battery draining completely. But such a facility is yet to be implemented at many places which create a range fear within EV users. This paper proposes a vehicle to vehicle fast charging (V2V) on such an occasion. An EV charger consists of a power converter and a communication section that communicates with the EV using a standard charge protocol. At present there are three protocols followed internationally for fast charging: CCS of European Union, CHAdeMO of Japan and GB/T of China. Fast charging requires to access fast charging port. Power can neither be drawn nor supplied to the port without proper protocol. There is no standard protocol devised for this purpose at present. We propose to use the standard available charge protocol (G2V) and vehicle to grid (V2G) protocols for the V2V charging. Here we have used CHAdeMO for demonstration. The vehicle could be fast charged from another vehicle during an emergency.

Keywords. Electric Vehicles, ON-Board charger, DC Fast Chargers, vehicle fast charging, CHAdeMO

1. INTRODUCTION

Increasing population of Electric Vehicles has placed a high demand for the charging infrastructure and related services. During a breakdown of an EV due to discharge of the battery, the vehicle has to be either charged from a mobile EV charger or has to be pulled to the nearest charging station/ workshop by a rescue vehicle. It consumes a lot of time if this happens on a highway before the vehicle could reach the nearest charge station. It will be of great relief and anxiety free travel, if there is a hand held Emergency Vehicle to Vehicle (V2V) fast charger. The broke down vehicle can be charged from a passing vehicle using this V2V charger within a matter of minutes. Fast Charging requires establishing charging with few digital interfaces between charger and vehicle and a serial communication interface through CAN bus using charge Protocol specific to that vehicle. Once communication is established, the charge current has to follow the continuous command from the vehicle through the CAN bus. Presently there are three standard charge protocols are followed internationally. CHAdeMO protocol by Japan is the forerunner, followed by GB/T of China and CCS of European Union. CHAdeMO has devised other protocols to utilize the charged battery of the EV, such as Vehicle to Home (V2H), Vehicle to Building (V2B), Vehicle to Grid (V2G), Vehicle to Load (V2L) grouped under V2X. All these protocols can be used to draw power from the battery pack. CCS too has V2G protocol to discharge the charged EV to grid. This can be used to export power to the grid during peak demand period and make a earning out of it. It is proposed to use the either V2G or V2H protocols for drawing power from a charged vehicle, say donor vehicle (DV) to charge the drained vehicle, say receptor vehicle (RV) using the charge protocol G2V.

Wireless charging is proposed [1] for V2V charging. Different coil designs are compared and different resonant options are analyzed. Power Capacity calculation and Energy cost calculation with EV as a source is provided. This calls for additional modules to be built within the vehicle for charging, communicating and supervisory control. Wireless charging has its own disadvantages like capacity limitation, distance of transmission and alignment. Bidirectional converter is proposed [2]. Its topology and operation in different modes are discussed which is additional to the On-Board charger present in the vehicle.

Several V2V charging strategies are proposed in [3]. One is Conventional way of exporting (V2G) and importing power (G2V) with the grid as an intermediate platform, utilizing the Bi-directional ON-Board charger (BDOBC) of the vehicle. The second one is eliminating this intermediate platform and charging the vehicle directly. Many EV's are presently equipped with Uni-directional chargers. Hence this strategy can be utilized only with few vehicles that are equipped with BDOBCs. For V2G capability, BDOBCs should have current source capability, while for V2H or V2B it should have voltage source capability at the AC end. Third one is bypassing the DC/AC of the donor and AC/DC of the receptor ON-Board charger (OBC), and connecting the DC sections directly. This case is plausible if only there is a double conversion. Additionally a provision for taking DC out is required and should have an additional outlet. This is also risky as the DC may not come with short circuit protection. The fourth one is an Off-Board DC V2V, which has a better feasibility and can be fast too. V2V charging is proposed [4] using a control algorithm incorporated in the BDOBC and a communication network between EV's to be established by a MQTT protocol over TCP/IP. A MQTT client mobile application is used for monitoring and control. Wireless Power Transfer (WPT) based V2V charging is proposed [5]. This requires additional hardware on all the vehicles. Communication methodology is
ambiguous. It discusses more on the angular offset of the WPT coils.

Various topologies suitable for V2G and V2H are discussed in length and are compared [6]. Communication standards used for such applications are also discussed. Factors like driving range distribution, optimal charge capacity for public charging infrastructure, charging methodology to minimize battery degradation were studied and analyzed for CHAdeMO quick charging station [7]. Power output capability and its duration when used in V2H mode were analyzed with PEV and PHEV based on the residential energy data collected [8]. Opportunities for V2H, V2G and V2V technologies were studied and challenges associated with it were analyzed [9]. Framework for operations under these technologies, modeling of household electrical appliances, study of power electronic devices and battery technologies are also carried out.Multiple protocols like Chademo, CCS Combo are analyzed in implementation of dynamic DC charging [10] and SAE J1772 based V2X AC charging where EV is charged through intermittent renewable energy source.

2. PROPOSED METHODOLOGY

DC charging through the Fast Charging port is proposed for V2V emergency charging. Donor vehicle shall use any of the V2X protocol to borrow energy from Chademo based vehicles and V2G protocol from CCS. On the receptor side G2V charge protocol is used for DC fast charging from the DV. An external charger shall be used for this purpose. The charger consists of a Power Module with two fast charge connectors and a controller as shown in Figure 2.1 for interfacing and communicating between the vehicles and two sets of high voltage relays one at the input and other at the output. One connector shall be connected to the input relay and the other to the output relay. The fast charge connectors shall be of Chademo or CCS depending on the protocol followed by the vehicle. Chademo connector has power, digital interface and CAN communication connections, while CCS has power, PWM control pilot interface, proximity and Power Line Communication (PLC) over the control pilot. The controller needs to have necessary digital and communication interfaces.

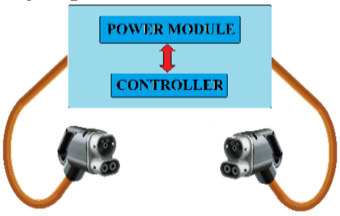

Figure 2.1. Proposed V2V Emergency DC Fast Charger

3. POWER MODULE

The charger is intended to charge similar type of vehicles that have similar battery voltages and capacity. Cars in India use low voltage of 72V while all other countries use 350V Battery. Generally Car battery capacity ranges from 20 to 50 kWH (50-120AH). So the output current requirement varies from 50A for 20kWH to 120A for 50kWH to support 1C charging. Here let us select an output current of 80A to suit most of the applications and at the same time keep the converter size minimum. A buck converter is best suited for this application. Isolation is not warranted as it is between two battery packs. Being a medium voltage application either an IGBT or a MOSFET can be selected. With MOSFET, high switching frequency can be achieved without increasing the losses greatly thereby reducing the inductor requirement. The main disadvantage is many devices are to be paralleled. Whereas a single device can be selected if IGBT is used, but the switching frequency has to be low enough to contain the losses associated with it thus increasing the inductor size. TABLE I specifies the brief input and output requirements of the converter. Detailed design is provided for all the power components.

TABLE I. Design parameters

V_{in}	300 – 399 V (351.5V Nominal)
V_o	300 – 399V
I_o	80A
P_o	32 KW
f_{sw}	30 kHz

3.1. Inductor Design

Inductor value is calculated based on the minimum duty cycle and the ripple current and is designed using an amorphous core. Let us assume 10% ripple, i.e., 8A and the peak to peak ripple current

$\Delta IL = 16A$.

Minimum duty cycle

$$\delta_{T\min} = \frac{V_{o\min}}{V_{i\max}} = \frac{300}{399} = 0.75 \tag{3.1}$$

Inductance

$$L \geq \frac{V_{o\min}(1-\delta_{T\min})}{\Delta I_L f_{sw}}$$

$$\geq \frac{300(1-0.75)}{16 \times 30e^3} \geq 156.25\mu H \tag{3.2}$$

$$E = \frac{1}{2}LI^2 = \frac{1}{2} \times 156 \times 10^{-6} \times 80^2 = 0.499J \tag{3.3}$$

Let us select FS-520026-2 FluxSan Fe-Si Alloy Powder core from Micrometals. The core is selected based on the required geometry and the energy storage needs. The dimension and magnetic data are given in TABLE II. Figure 3.1 provides the Energy handling capability, Figure 3.2 gives core loss information and Figure 3.3 provides the Inductance factor AL.

TABLE II. Core parameters

OD	132.54 mm	ID	78.59 mm	HT	20.32 mm
L_e	32.429 cm	A_e	5.35 cm^2	V_e	173 cm^3
SA	515 cm^2	μ_i	26	A_L	54 nH±8%

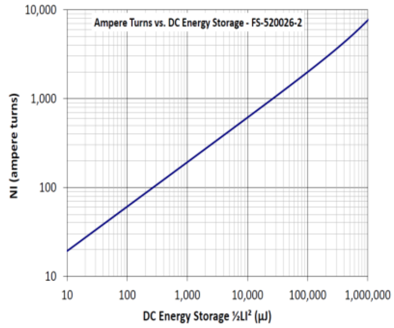

Figure 3.2. Energy vs Amp-Turns

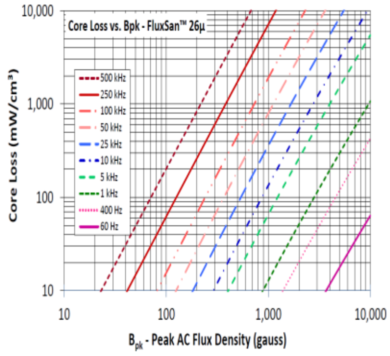

Figure 3.2. Energy vs Amp-Turns Flux Density vs Core Loss

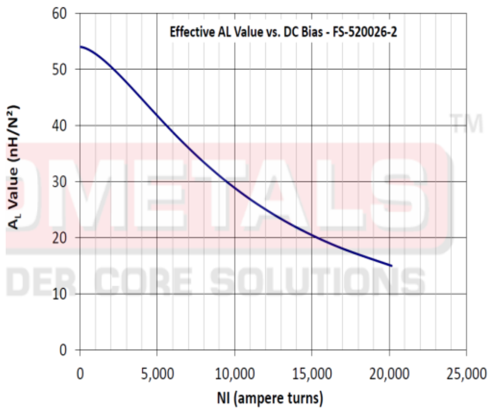

Figure 3.3. Amp Turns vs AL

Number of turns

$$N = \sqrt{\frac{L}{A_L}} = \sqrt{\frac{156 \times 10^{-6}}{42 \times 10^{-9}}} = 61T \tag{3.4}$$

Operating flux density

$$B_{ac} = \frac{L\left(\frac{\Delta I}{2}\right)\times 10^{-4}}{A_e N}$$
$$= \frac{156\times 10^{-6}\times 8\times 10^{4}}{5.35\times 61} = 0.038 Tesla \quad (3.5)$$

From Figure 3.1 core loss is around 50mW/cm3 for 30 kHz at 0.038Tesla.
Therefore core loss = 50mW/cm3 x 173cm3 = 8.65W.
Let us choose 8 SWG copper wire 2 numbers in parallel.
Current density = 81.5/(2x12.97)=3.14A/mm2
Wire resistance =0.764mΩ/m x 8.479m = 6.478mΩ
Cu Loss =81.52 x 6.478 x 10-3 = 43W
Total loss = 51.678W
Temperature rise

$$\Delta T = \left(\frac{P}{SA}\right)^{0.833}$$
$$= \left(\frac{51.678\times 10^{3}}{515}\right)^{0.833} = 46.47^{o}C \quad (3.6)$$

Where P is power loss in mW and SA is the total surface area in cm3.

3.2. Device Selection

Let us select FCH023N65S3 MOSFET from ON Semiconductor. It is rated for 75A at 650V and has an RDS(ON) of 23mΩ. Let us use 7 nos in parallel to maintain low loss and operate under safe limits.

Conduction loss

$$P_{Trc}\,@25^{o}C = I_o^2 R_{DS(ON)}\delta_{T\min}$$
$$= 80^2\times\left(\frac{0.023}{7}\right)\times 0.75 = 15.77W \quad (3.7)$$

$$P_{Trc}\,@100^{o}C = 15.77W\times 1.75 = 27.6W \quad (3.8)$$

Switching loss

$$P_{Trs} = \frac{1}{2}VI(t_r + t_f)f_{SW}$$
$$= \frac{1}{2}\times 400\times 80\times(55+29)\times 10^{-9}\times 30\times 10^{3}$$
$$= 40.32W \quad (3.9)$$

Total device loss = PTrc + PTrs = 67.92W

Junction to Case thermal resistance RθJC =0.21oC/W per device and RθCS =0.24oC/W per device.
Therefore for 7 devices in parallel RθJC =0.03oC/W and RθCS =0.0343oC/W.

$$T_J = P\left(R_{\theta JC} + R_{\theta CS} + R_{\theta SA}\right) + T_A \quad (3.10)$$

Heat sink thermal resistance

$$R_{\theta SA} \le \frac{T_J - T_A}{P} - R_{\theta JC} - R_{\theta CS} \quad (3.11)$$
$$\le \frac{125-50}{67.92} - 0.03 - 0.0343 \le 1.039$$

3.3 Diode Selection

Let us choose DSEI 6006A diode from IXYS, 3 in parallel. The diode is rated for 60A at 600V and has a reverse recovery time of 35ns.

Conduction loss

$$P_{Dc} = IV_f(1-\delta_{T\min}) \tag{3.12}$$
$$= 80 \times 1.3 \times 0.25 = 26W$$

Switching loss

$$P_{Ds} = Q_{rr}V_R f_{SW}$$
$$= 2.5\times10^{-6} \times 300 \times 30\times10^{3} = 22.5W \tag{3.13}$$

Total diode loss = PDc + PDs = 48.5W

Junction to Case thermal resistance RθJC =0.75oC/W per device and RθCS =0.25oC/W per device. Therefore for 3 devices in parallel RθJC =0.25oC/W and RθCS =0.0833oC/W.

$$T_J = P(R_{\theta JC} + R_{\theta CS} + R_{\theta SA}) + T_A \tag{3.14}$$

$$R_{\theta SA} \le \frac{T_J - T_A}{P} - R_{\theta JC} - R_{\theta CS}$$
$$\le \frac{125-50}{48.5} - 0.25 - 0.0833 \le 1.213 \tag{3.15}$$

3.4 Efficiency Estimation

Inductor loss = 51.678W
MOSFET loss = 67.92W
Diode Loss = 48.5W
Other losses = 20W
Total loss = 188.09W
Output power = 400 x 80 = 32000W
Input power = 32000W + 188.09W=32188.09W
Efficiency η = 99.415%

4. COMBINED CHARGING SYSTEM(CCS) PROTOCOL

Combined Charging System (CCS) is a globally supported standard for communication and charging of battery-powered electric vehicles. Two different types of connectors are under use, Combo1 with Type I AC charging for US and Combo 2 with Type II AC charging for Europe based on J1772/IEC62196-3 standards as can be seen in Figure 4.1.

Figure.4.2 shows connection details. Verification of the status is carried out by a PWM signal generated by the CP and further communication is through a TCP/IP based 7 layer OSI model High Level Communication (HLC) as shown in Figure.4.3

Figure 4.1.Combo 2 Plug and Socket

DC+ DC Power
DC- Output
CP – Control Pilot

PP – Proximity Pilot
PE – Power Earth
Lx – AC Phase x (1,2,3)
N – Neutral articles.

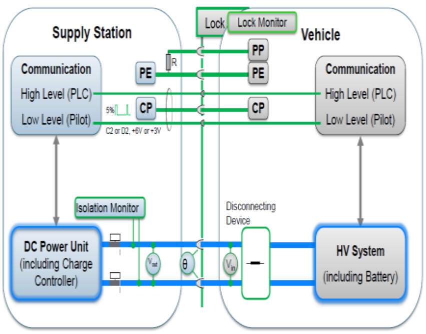

Figure 4.2.CCS Charging Architecture

The link is established by Power Line Communication (PLC) using HomePlug Green Phy physical layer. The charge process sequence starts with 5% PWM signal at 1 kHz to trigger the HLC. The amplitude of the PWM is modified by the EV which is an indication of the status such as

a. Vehicle not connected – State A (12V)
b. Vehicle connected but not ready to charge – State B (9V)
c. Vehicle connected and ready to charge – State C (6V)
d. Ventilation required – State D (3V)
e. Fault – State E (0V)
f. Electric Vehicle Supply Equipment (EVSE) not available – State F (-12V)

Once it attains State C, EV proceeds to establish HLC. This being a high-frequency signal, there is a possibility that it might skip the limits of private electrical network resulting into a cross talk. To ensure only physically connected EV and EVSE join a common AVLN, Signal level Attenuation Characterization (SLAC) protocol is used. EV sends sounding packets as broadcasts to all the charging stations on the same electrical network. SLAC measures the attenuation between two PLCs. PLC modules that exhibit the lowest attenuation to each other is physically connected. Once it is ensured EVCC uses SECC Discovery protocol to obtain the IP address and port number of SECC. Then TCP/IPv6 is setup. The communication sequence starts with the following Application Layer messages.

a. SupportedAppProtocolReq/Res

Request and response of the protocol compatibility.Either DIN Spec 70121 or ISO 15118.

b. SessionSetupReq/Res

Establishes communication session and exchanges client-server IDs.

c. ServiceDiscoveryReq/Res

Selects a Service. Charging, Discharging the EV are all some of the services offered by the EVSE.

d. ServicePaymentSelectionReq/Res

Selects the payment method

e. ContractAuthenticationReq/Res

Verifying Contract Authentication

f. ChargeParameterDiscoveryReq/Res

Verifies the compatibility of charging parameters

g. CableCheckReq/Res

For insulation verification

h. PreChargeReq/Res

Initial charging

i. PowerDeliveryReq/Res

For pre-charging

j. CurrentDemandReq/Res

Charge current request

k. PowerDeliveryReq/Res

For charging

l. WeldingDetectionReq/Res

Checks for welding of contactors

m. SessionStopReq/Resnames

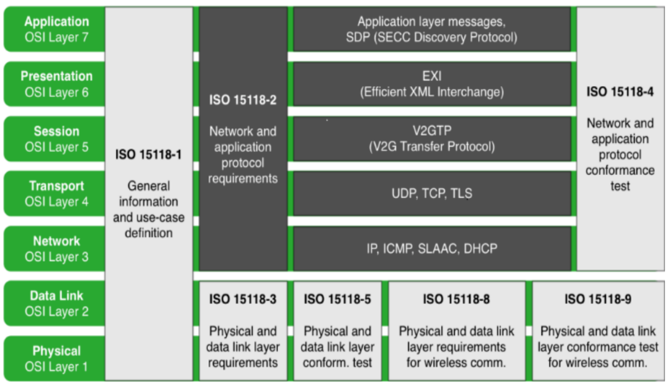

Figure 4.3.OSI Layer Model and Standards for HLC

At the end of the session the 5% PWM signal is switched off to terminate the process. All the application layer messages are defined using XML and has a specific time out values. These messages are converted into binary data by Efficient XML Interchange (EXI) codec employing the XSD file.Chademo Protocol.

Chademo unlike CCS communicates through a CAN bus and have few digital interface as can be seen in Fig.8. The control ground to the charger is obtained from the EV side On-board auxiliary battery. The extension of ground is sensed to perform the

Connection check. The charging sequence is shown in Figure 4.4. Switching ON 'd1' sends start-of-charge signal by extending 12V and EV recognizes it by 'f' on. It responds by sending the battery parameters through the CAN bus. The compatibility is verified by the charger and it transmits the charger parameters. EV does the compatibility check and start permission is given by turning on 'k' which is sensed at 'j' by the charger. Connector lock is activated and insulation check is carried out. Charging ready signal is generated by activating 'd2' and EV recognizes it through 'g' and closes the EV contactor. The EV side contactor coil is powered by the charger side auxiliary power source. The EV gives current request based on the battery condition and the charger follows by supplying the requested current. The charging continues till the stop condition is reached.

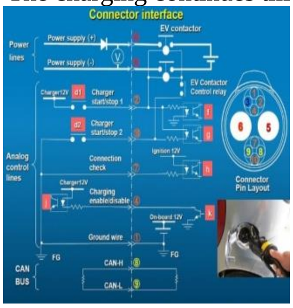

Figure 4.4. Chademo Charging Sequence

Once the battery is fully charged or the stop condition is reached, EV reduces the current request to zero. EV turns off the contactor once the charging current drops to zero and activates stop command by turning off 'k'. In turn the charger terminates the session by de-activating 'd1' and 'd2'. Finally the lock is released.

The data is transmitted at the rate of 500 bps. There are 5 data frames associated with the main charging process. Three are from the EV and two are from the EVSE. An example of the data frames during a charging process is given below in Table III. The first three data frames in yellow represents the EV data and the other two in green represents EVSE. Both the message IDs and data are in Hex format. DLC is the data length.

TABLE III. Data frames during charging

ID	DLC	D0	D1	D2	D3	D4	D5	D6	D7
100	8	0	0	0	0	A9	1	FA	0
101	8	0	FF	3C	0	0	0	0	0
102	8	1	A4	1	50	0	1	5B	0
108	8	1	8F	1	50	2C	1	0	0
109	8	1	45	1	80	0	5	FF	2D

5. HARDWARE

A practical working model is built employing Chademo protocol. Circuit schematic of the Buck Converter used for charging is shown in Figure 5.1. Q1 has seven numbers of discrete MOSFETs (FCH023N65S3) with individual gate resistors for turn-on and turn-off. D9 is the freewheeling diode and it has three numbers of DSEI 6006A connected in parallel. Inductor L1 is wound on FS-520026-2 torroidalFluxSan Fe-Si alloy powder core. The power circuit and its driver are assembled on a PCB. Discrete Mosfet based driver is used considering the drive requirement. A hall effect CT CT1 is used to measure and control the charge current. C6 and C7 constitute the output filter capacitor while C4 is the input filter capacitor. C7 is a Poly propylene capacitor that has low ESR and ESL to attenuate high frequency ripple and switching noises. Input and output voltages are measured using resistor chains. Two temperature sensors U1 and U2 are used to measure the device temperature and are utilized in monitoring and de-rating control. A controller using Microchip's dsPIC33FJ64GS606 is used for both the charge control and RV side communication. MCP2532 is used as CAN transceiver. For DV additional controller is used. Both the controllers exchange data through UART

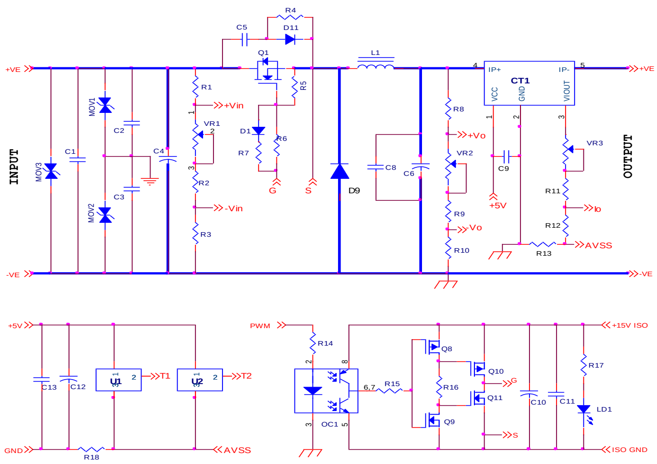

Figure 5.1. Circuit Schematic

6. RESULTS AND CONCLUSION

Due to difficulty in getting the vehicles for testing, the charger is tested on a resistive load for 80A at 350V. The measured efficiency is 99% and is close to the estimated value. The digital interface is simulated using switches and the vehicle CAN messages are transmitted from a CAN analyzer and the protocol is verified.

At this rate of charging a car with 20 kWh battery pack whose range is 100 km can charge to 30% of its capacity in around 13 minutes, which is sufficient to cover 30 kms. This charge is more than sufficient to reach the next charging station. Vehicles with higher capacity have more range. Therefore it is sufficient to charge it to a lower capacity to reach the same distance. So the charging time will remain almost constant irrespective of the vehicles battery capacity assuming similar efficiency. Assuming a distance of 25 km between two charging station, the distance to travel the nearest one is only 12 km. charging time of around 13 minutes is highly convenient for the acceptor and is quite.

7. REFERENCES

[1] XiaolinMou, Rui Zhao,Daniel T Gladwin, "Vehicle-to-Vehicle charging system fundamental and design comparison",IEEE International Conference on Industrial Technology (ICIT), Feb.2019

[2] Sai Krishna Vempalli, K Deepa,Prabhakar.G,"A Novel V2V Charging Method Addressing the Last Mile Connectivity", IEEE International Conference on Power Electronics Drives and Energy Systems (PEDES), 2018.

[3] XiaolinMou, Rui Zhao, Daniel T Gladwin, "Vehicle to Vehicle Charging (V2V) Bases on Wireless Power Transfer Technology", IECON, Oct 2018.

[4] SeyfettinVadi et al, "A Review on Communication Standards and Charging Topologies of V2G and V2H Operation Strategies", 12, 3748, Energies Sept. 2019

[5] TakafumiAnegawa, "Characteristics of CHAdeMO Quick Charging System", World Electric Vehicle Journal, vol. 4, pp.818-822, Nov. 2010 WEVA.

[6] VitorMonteiro et al, "Improved Vehicle-to-Vehicle (iV2H) Operation Mode: Experimental Analysis of the Electric Vehicles as Off-Line UPS", IEEE Transactions on Smart Grid,vol 8, Issue 6, pp. 2702-2711, Nov 2017.

[7] Photovoltaic based Induction motor speed control Using SEPIC converter" International Journal of Advanced Science and Technology, Vol. 29, No. 10S, (2020), pp.3932-3945

[8] David P. Tuttle et al,"Plug-In Vehicle to Home (V2H) Duration and Power Output Capability",IEEE Transportation Electrification Conference and Expo (ITEC), June 2013

[9] Chunhua Liu et al, "Opportunities and Challenges of Vehicle-to-Home, Vehicle-to-Vehicle and Vehicle-to-Grid Technologies", Proceedings of the IEEE, vol. 101, Issue: 11 , pp. 2409 – 2427, Nov. 2013.

[10] Gautham Ram Chandra Mouli et al, "Implementation of Dynamic Charging and V2G using Chademo and CCS/Combo DC charging standard",Transportation Electrification Conference and Expo (ITEC), June 2016.

[11] Shanmugasundaram, N., Thangavel, S."High frequency power cable modeling for screen voltage calculation of different cable length with induction motor drive system (VFD)"ARPN Journal of Motorering and Applied Sciences, 2015, 10(20), pp. 9150–9158

[12] Shanmugasundaram, N., Thangavel, S."Modeling and simulation analysis of power cable a three level inverter fed induction motor drive"Journal of Computational and Theoretical Nanoscience, 2017, 14(2), pp. 972–978.

[13]. N. Shanmugasundaram, K. Sushita, S. Pradeep Kumar and E.N. Ganesh "Genetic algorithm-based road network design for optimising the vehicle travel distance" Int. J. Vehicle Information and Communication System, Vol. 4, No. 4, 2019.

[14]. K.Sushita, N. Shanmugasundaram "Performance Analysis of Solar operated BLDC motor" International Journal of Advanced Science and Technology, Vol. 29, No. 7, (2020), pp. 1517-1527.

[15]. K.Sushita, N. Shanmugasundaram "Performance of BLDC motor with PI,PID and Fuzzy Controller" European Journal of molecular and clinical medicine, Vol. 7, No. 8, (2020), pp. 2510-2524.

[16]. K.Sushita, N. Shanmugasundaram "Performance and Comparative Analysis of Bldc Motor with Pi and Pid Controllers" Annals of the Romanian Society for Cell Biology, Vol. 25, Issue 3, 2021, Pages. 219 – 228.